

2018



**25th Congress of
International Federation for
Heat Treatment and Surface Engineering**

11-14 September 2018 | Xi'an China

PROCEEDINGS



Organized by Chinese Heat Treatment Society (CHTS)

25th IFHTSE CONGRESS PROCEEDINGS

11-14 September 2018

Xi'an China



Chinese Heat Treatment Society

Tel: +86 (0) 10 6292 0613 • Email: chts@chts.org.cn • Web: www.chts.org.cn

Add: 18 Xueqing Rd., Beijing, China

| | |
|---|-----|
| based on terahertz time-domain spectroscopy..... | 451 |
| Al-modified 7YSZ thermal barrier coating prepared by PS-PVD and its application prospect..... | 452 |
| The evaluation of durability of plasma-sprayed thermal barrier coatings with double-layer bond coat..... | 454 |
| Effect of particle size on the cracking behavior of plasma-sprayed YSZ coatings during thermal shock and erosion testing..... | 455 |
| Sintering mechanism of plasma-sprayed TBCs-from free-standing to constrained states..... | 456 |
| Structurally integrated damage tolerant coatings..... | 457 |
| Tailoring porous structures of nano zinc oxide coatings by liquid plasma spraying for enhanced photocatalytic performances..... | 457 |
| Mechanical properties of in-situ micro-forging assisted cold spray additively manufactured AA6061 alloy..... | 458 |
| Influence of the temperature on the microstructure and wear performance of HVOF sprayed bimodal WC-12Co coatings..... | 458 |
| Suspension plasma spray fabrication of black titanium dioxide photocatalytic coatings with visible light absorption performances..... | 459 |
| Development of a FeCrMnBC-based economical wear and corrosion resistant coating..... | 459 |
| Optimization of spray parameters on the corrosion behavior of HVOF sprayed Fe-based amorphous coatings..... | 460 |
| Microstructure and wear behavior of Al _{0.6} TiCrFeCoNi high entropy alloy coating produced by HVOF..... | 460 |
| Detonation spraying of the copper powder coated with graphene..... | 461 |
| Microstructure and properties of laser re-melting FeCoCrNiAl _{0.5} Si _x high-entropy alloy coatings..... | 461 |
| Surface nanocrystallization of AZ91D magnesium alloy by cold spraying shot peening..... | 462 |
| Preparation and flowability of shell-core-structured graphite-gray cast iron powder for thermal spray application..... | 462 |
| A highly porous thermal barrier coating based on Gd ₂ O ₃ -Yb ₂ O ₃ Co-doped YSZ..... | 463 |
| A novel non-parabolic kinetic model for long term oxidation of MCrAlY bond coat..... | 463 |
| Thermal shock resistance of thermal barrier coatings with different shapes processed by laser..... | 464 |
| Evaporation of small droplets in plasma spray-physical vapor deposition based on plasma heat transfer..... | 464 |
| Hot corrosion behavior of NiCrB coating sprayed by wire arc thermal spraying..... | 465 |
| Research on crack failure modes of thermal barrier coatings based on acoustic emission technique..... | 466 |
| In situ synthesis of TiN reinforced Fe-based amorphous coating by reactive plasma spraying..... | 467 |
| The tribological and electrochemical behavior of HVOF sprayed WC-10Co-4Cr coatings..... | 467 |

Frictional and Wear

| | |
|--|-----|
| A novel low friction phenomenon in gradient nano-grained CuAg alloy..... | 468 |
|--|-----|

| | |
|---|-----|
| Influence of nitride and multiple peening on surface characteristic of AISI D2..... | 469 |
| Correlation between microstructure evolution, strain-hardening in friction-induced deformation layer and wear behavior of 40Cr steel..... | 470 |
| Tribological properties of thermally sprayed WC-10Co-4Cr coatings with nano-additives..... | 472 |
| Wear behaviors of the arc-sprayed FePSiB-based amorphous and nanocrystalline coatings..... | 473 |
| Influence of grit dimension on the friction and wear behavior of CT80 tubing..... | 474 |
| Friction and wear behavior of H13 steel processed by laser surface remelting..... | 475 |
| Comparative study on microstructures and tribological properties of the sulfurizing layers prepared on different cladding coatings..... | 476 |
| Abrasive wear of an advanced medium Mn transformation induced plasticity steel..... | 477 |
| Surface microstructure evolution of CL65 in wear..... | 477 |
| A wear trend forecasting model of gas turbine ongoing research based on optimized genetic algorithm and improved bp neural network..... | 478 |
| Tribological properties of plasma sprayed Al ₂ O ₃ -TiO ₂ coatings with nano graphite..... | 478 |
| Study on strengthening wear resistance and friction reducing of epoxy composite coatings..... | 479 |
| Finite element analysis of non-linear contact wear of U-shaped ring of power tools..... | 479 |
| Sliding wear behavior of nano-structured Al ₂ O ₃ -YSZ coatings fabricated by plasma spraying..... | 480 |
| Friction and wear properties of argon arc cladding Ni-based nanocrystalline coatings..... | 480 |
| Influences of yttrium addition on the porosity reduction and tribological properties of (W, V, Ti)C-8%Co cemented carbide alloy..... | 481 |
| Influence of the cementite morphology on rolling wear of D2 wheel steel..... | 481 |
| Research on friction and wear properties of quenching partitioning-tempering steel..... | 482 |
| Effect of cryogenic treatment on mechanical properties and microstructure of 42CrMo after thermo-mechanical processing..... | 483 |
| Study on dry sliding friction-induced deformation layers at different wear stages of 30CrMnSi steel and its wear behavior..... | 484 |
| Microstructure and tribological properties of micro-arc oxidation TiO ₂ coating before and after SiC particles incorporation..... | 486 |
| Erosion test of electroless deposited Ni-Fe-P alloy coatings..... | 487 |
| Effect of different heat treatment time on wear performance of Al ₂ O ₃ -13wt%TiO ₂ coating..... | 488 |
| A highly porous thermal barrier coating based on Gd ₂ O ₃ -Yb ₂ O ₃ Co-doped YSZ..... | 489 |
| Development of a FeCrMnBC-based economical wear and corrosion resistant coating..... | 489 |
| Study on the transfer behavior of polyimides adding aluminum rubbing with Ti-6Al-4V alloy at different temperatures..... | 490 |
| Effect of nano-additives containing rare earth oxides on impact abrasive wear behavior of high chromium cast irons..... | 490 |
| Effect of flow velocity on erosion-corrosion rate of mild steel in solid-liquid two phase fluids comprising CO ₂ and Cl ⁻ environments..... | 491 |
| Research on laser surface strengthening of U71Mn steel based on resistance of the sand erosion..... | 491 |

| | |
|--|-----|
| Elevated temperature wear behaviour of rare earth modified WC12Co coating..... | 492 |
| Effect of mechanical alloying speed on properties of CNTs-SiC/Ni laser cladding coating..... | 492 |

Modelling and Simulation

| | |
|--|-----|
| Numerical simulation of heat treatment and its engineering application..... | 493 |
| Heat treatment simulation for low pressure super carburizing process..... | 494 |
| Heat transfer coefficient model of large cross section steel bar during water cooling process..... | 495 |
| Modelling on quenching precipitation of Al-Cu-Cd alloy..... | 496 |
| Diffusion simulation in SUS 430 stainless steel interconnect with a MnCu coating at 800 °C..... | 497 |
| Application of universal function approximator to predict HTC during quenching..... | 498 |
| Influence of circular workpieces configurations on temperature field of vacuum heating process..... | 498 |
| Heat transfer, microstructure evolution and stress development in a quenched 403 stainless steel forging..... | 499 |
| Microstructural evolution of a steam turbine rotor subjected to a water quenching process: numerical simulation and experimental verification..... | 499 |
| Modeling carburization heat treatment processes of steel camshaft in marine engine using commercial software DANTE..... | 500 |
| Superalloy in synchronization powder feeding laser cladding..... | 500 |
| Microstructure-based mesoscopic modeling of deformation behavior of dual-phase steels using crystal plasticity finite element method..... | 501 |
| Effect of residual stress on indentation and rebound hardness measurement..... | 502 |
| Isothermal phase transition kinetics of TC11 titanium alloy..... | 504 |
| Stress relaxation performance and thermal calibration of TC4 titanium alloy at high temperature..... | 506 |
| Numerical and experimental investigation into the austenite decomposition kinetics of 50Cr5NiMoV steel..... | 508 |
| Three-dimensional numerical simulation of temperature field of Ni based cellular automaton modeling of nitriding process in pure iron..... | 509 |
| Design method fin-tube heat exchange based on numerical simulation..... | 509 |

Characterization and Evaluation of Residual Stress; Shot Peening Technology

| | |
|--|-----|
| Evaluation of internal residual stress in rolled pure copper plate..... | 510 |
| Effect of laser shock processing and aluminizing on microstructure and high temperature creep properties of 321 stainless steel..... | 511 |
| Research progress and application of residual stress neutron diffractometer at CMRR..... | 512 |
| Investigation on the thermostability of residual stress and microstructure in shot peened SAF 2507 duplex stainless steel..... | 513 |
| Evaluating the fatigue cracking risk of surface strengthened 50CrMnMoVNb spring steel with abnormal life time distribution..... | 514 |

A novel low friction phenomenon in gradient nano-grained CuAg alloy

Zhong Han

(Institute of Metal Research)

Abstract: Metallic materials usually exhibit high coefficients of friction (COFs) under dry sliding, generally ranging from 0.6 to 1.2. The primary reason responsible for high COFs in metals is sliding-induced plastic deformation of near-surface material, especially for ductile metals under high loads. During sliding, local asperity contacts cause accumulated plastic straining that makes the near-surface material susceptible to shear instabilities, triggering surface roughening via micro-cracking or folding that unavoidably elevates the COFs. Repeated sliding on the roughened surface may generate wear particles and lead to mechanical-alloying and cold-welding of the particles with the wear surface, compounded with other mechanisms, facilitating formation of nano-structured tribo-layers (or mechanical mixing layers). Delamination of these brittle tribo-layers in subsequent sliding contributes to further surface roughening and COF elevation. Hence, suppressing surface roughening and formation of delaminating tribo-layers in the sliding surface are crucial for lowering COF of metals.

In fact, lowering COF of metals is of great technological significance for improving the reliability and efficiency of metal contacts in engineering applications ranging from gears to automobile cylinders, although it is technically challenging. Unlike other mechanical properties, COF, a parameter describing the state of contact of bodies in a tribo-system, is insensitive to microstructure modifications of metals. For instance, Refining metals' grains into the nano-scale raises their hardness by many times, but does not obviously reduce COF either in pure metals (Ni, Ti, Al, and Cu or alloys), especially under high-load sliding. This arises from the fact that nano-grained (NG) metals possess very limited plastic deformation ability so that strain localization occurs adjacent to the sliding interface, triggering surface roughening and formation of delaminating tribo-layers. Clear correspondences between high COFs and formation of delaminating tribolayers were also observed in NG metals.

Recently, gradient nano-grained (GNG) structures, a NG layer forming on a coarse-grained (CG) substrate with a graded variation of grain size in between, was found to be effective in suppressing strain localization and accommodating very large plastic strains prior to failure. More importantly, the GNG structures are capable of suppressing surface roughening in metals undergone large plastic straining. In this work, we discovered that a submillimeter-thick stable gradient nano-grained surface layer enables a significant reduction in the COF, from 0.64 (CG sample) to 0.29, in a Cu-5Ag alloy under high-load dry-sliding with substantial plastic deformation of near-surface material. The unprecedented stable low COF originates from effective suppression of sliding-induced surface roughening and formation of delaminating tribo-layer. This novel low friction phenomenon thanks to the stable gradient nanostructures that can accommodate large plastic strains under repeated sliding for more than 30000 cycles. The finding seems to provide a strategy for lowering COFs of metals and alloys, in contrast to that with homogeneous structure refinements. The superior stability of the GNG structure against plastic deformation of near-surface materials during repeated sliding have been observed in other materials including pure copper and steel samples, which may find tremendous potential for technological applications in contact loading of metals.

Keywords: gradient nano-grained structure, Cu alloy, friction, surface deformation mechanism

Influence of nitride and multiple peening on surface characteristic of AISI D2

Koichiro Nambu¹, Masahiro Nishio¹, Jyunji Miyamoto², Masahiro Okumiya¹

(1. Toyota Technological Institute; 2. Daido University)

knambu@toyota-ti.ac.jp

Abstract: In recent years, weight reduction of automobiles is required from the viewpoint of global environmental problems. To achieve that requirement, the use of high tensile strength steels is increasing. Along with that, it is indispensable to increase the strength of the metal mold used for press working. The purpose of this research is to improve the wear resistance of the mold by hybrid surface treatment combining nitriding treatment and multiple peening treatment. In this composite treatment, it is possible to obtain an increase in hardness and residual stress by applying a peening treatment after the nitriding treatment, and further control of surface roughness and improvement in lubricity can be expected by multiple peening. AISI D2 was used for the test material. For nitriding treatment, plasma nitriding treatment was performed. In the multi-stage peening treatment, steel-based particles and alumina particles were used. A rolling friction test was conducted under no lubrication and the rolling friction coefficient was measured. AISI 52100 was used for the mating material for the rolling friction test. Fig.1 shows the rolling friction test results of the untreated material and the test piece treated only with steel type particles and the two-step processed test piece. Fig.2 shows the rolling friction test results of untreated material, nitrided material, test piece subjected to one step treatment after nitriding and test piece subjected to two-step treatment after nitriding treatment. From the results shown in Fig.1, it can be seen that the friction coefficient greatly decreases by applying the peening treatment. In addition, it can be seen that the two-stage treatment has a lower friction coefficient than the one-stage treatment. Improvement in hardness is considered to be a factor as a factor to obtain such a result. As a result of comparing the surface roughness of the first stage process and the second stage process, the surface roughness of the two-stage process is smaller. From this result, it is considered that the surface roughness is one of the factors affecting the rolling friction coefficient. From the results in Fig.2, it can be seen that the friction coefficient greatly decreases by nitriding treatment. However, the friction coefficient of the test piece subjected to the peening treatment after the nitriding treatment showed a tendency which was almost the same as that of the nitriding specimen. From these results, it was not possible to show the superiority by hybrid surface treatment under the current test conditions. On the other hand, in the two-stage peened treated material, it was possible to obtain the same decrease in friction coefficient as the nitriding specimen and it was shown that the two-stage peening process is effective for reducing the friction coefficient.

Keywords: nitriding, fine particle peening, hibrid surface treatment, friction coefficient

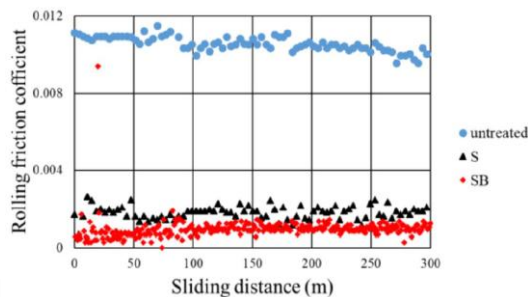


Fig.1

Fig.2

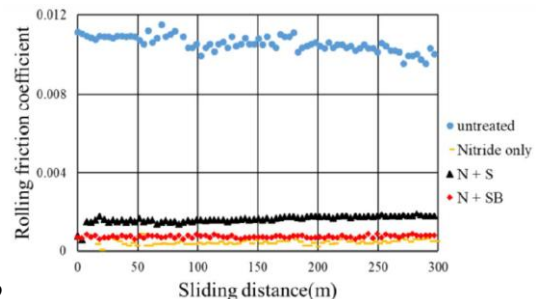


Fig.1 Rolling friction coefficient with no nitriding specimens

Fig.2 Rolling friction coefficient with nitriding specimens

Correlation between microstructure evolution, strain-hardening in friction-induced deformation layer and wear behavior of 40Cr steel

Shuang Liang¹, Peng Zhu¹, Jidong Zhu², Xing He¹, Yudan Yang¹, Wurong Wang¹, Xicheng Wei¹
(1. School of Materials Science and Engineering, Shanghai University, Shanghai 200444, China;

2. Zhejiang Jiajie Plastic Co., Ltd., Yiwu 322000, China)

wxc1028@staff.shu.edu.cn

Abstract: Microstructural evolution accompanied with changes of mechanical properties is generated in the tribolayer of friction pairs by the coupling effect of shear force and frictional heat during sliding contact. Such changes differing from the matrix may have a great effect on the tribological behavior of materials. Therefore, the objective of our present work is to study in detail about the microstructure evolution and strain hardening behavior in the surface/subsurface of widely used structural steel during friction and wear process.

A disk-on-pin configuration was used to carry out the unlubricated sliding wear tests. Normalized 40Cr steel and quenched tempered GCr15 steel were respectively employed as pin and disk materials. A normal load of 150 N and a sliding velocity of 0.56 m/s were selected. A series of tests were performed under different sliding distance conditions to study the evolution of wear behavior and subsurface structure. Coefficients of friction and wear rates were measured. Morphologies and chemical compositions of worn surface and subsurface were analyzed using scanning electron microscope and energy dispersive spectrometry. Plastic deformation and hardness changes in subsurface were characterized by 3D video microscope and Vickers hardness tester. Main results and conclusions are as follows:

- 1) Based on the variation of wear rate from Fig.1, the friction and wear behavior of 40Cr steel could be divided into three stages: running-in, slow wear and stable wear. During running-in stage, the worn surface was mainly featured by adhesion wear, with large spall at the same time; during slow wear stage, the wear behavior was mainly caused by delamination, significant adhesive and plastic flow traces were found in the worn surface; during stable wear stage, oxidative wear became the main wear mechanism due to high friction temperature.
- 2) During sliding process, pearlite and ferrite underwent dramatic plastic deformation along sliding direction and exhibited significant layered structures, lamellar structure parallel to the worn surface appeared on the outmost layer, as shown in Fig.2. The thickness of plastic deformation layer was in the range of 75-100 μm , depending on the sliding distance.
- 3) Fig.3 showed that a gradually decreased microhardness distribution was found in the deformation layer along the depth from worn surface, varied from more than 390 HV of the outmost layer to 200 HV of the matrix. Equivalent plastic strain also gradually decreased with increased depth from the surface. The plastic strain in subsurface could reach as high as 411% at the depth of 10 μm . Microhardness gradient and plastic strain gradient both showed the same trend that firstly increased and then decreased with the prolongation of sliding distance.
- 4) As shown in Fig.4(a), severe deformed vortex structure appeared in some local zones of the outmost worn subsurface as a result of shear instability at the stage of slow wear. Such structure exhibited relatively high microhardness of 505 HV owing to the dislocation hardening effect. It is assumed that the existence of vortex structure could improve the wear rate of 40Cr steel. Due to the comparatively high strain difference between vortex structure and lamellar flow structure, cracks initiated and tended to expand along the interface between such two structures with the prolongation of sliding distance (Fig.4(b)), then the vortex structure spalled and the lamellar structure transformed into vortex structure subsequently, these two processes went on repeatedly during the stage of stable wear.

Keywords: 40Cr steel, sliding wear, subsurface microstructure evolution, vortex structure

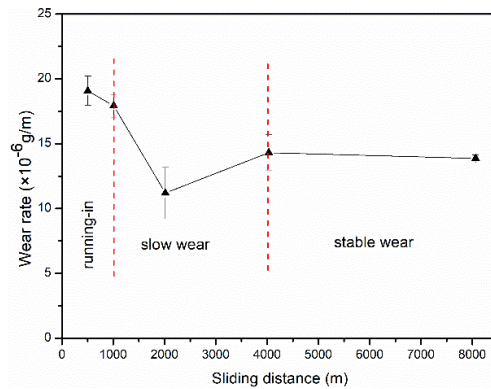


Fig.1 Wear rate of normalized 40Cr pin subjected to sliding distance

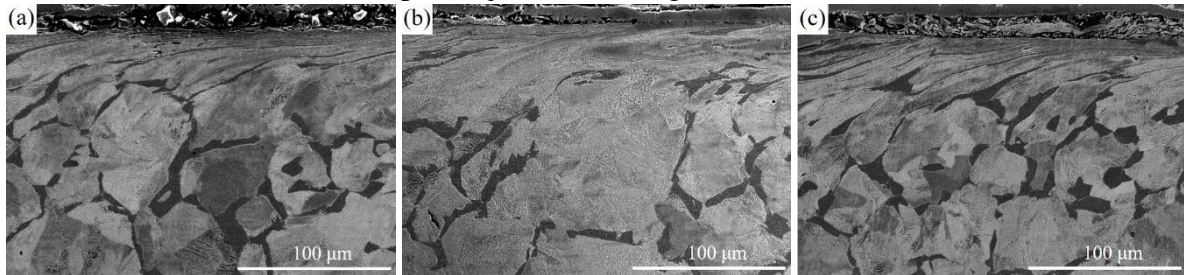


Fig.2 Cross-sectional microstructures of 40Cr after sliding: (a) 504 m; (b) 2016 m; (c) 8064 m

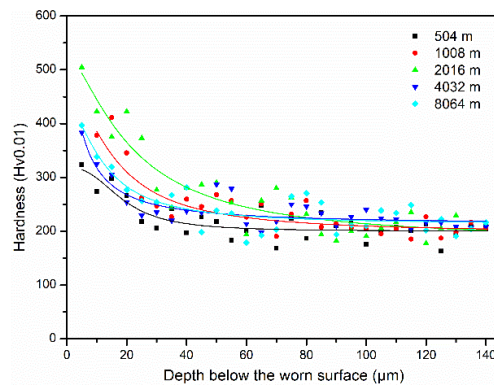


Fig.3 Variations of microhardness under the worn surface after different sliding distance

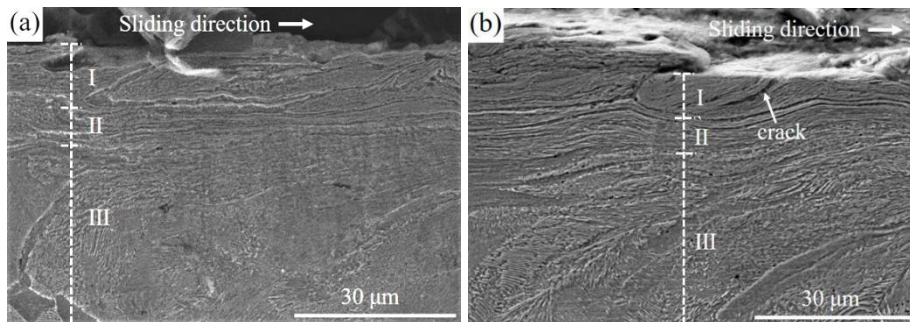


Fig.4 Illustration for typical outmost worn subsurface structures after sliding (a) 2016 m and (b) 8064 m (I : vortex structure; II : laminar flow structure; III: plastic strain structure)

Tribological properties of thermally sprayed WC-10Co-4Cr coatings with nano-additives

Xuewei Li¹, You Wang², Changhai Zhou¹, Zhizhong Zhu¹

(1. Heilongjiang University of Science and Technology; 2. Harbin Institute of Technology)

wangyou@hit.edu.cn

Abstract: WC-10Co-4Cr coating has good wear and corrosion resistance simultaneously, and is one of the common WC/Co(Cr) coatings. Though the Cr element is added into the coatings, the better corrosion resistance is not always maintained when the wear occurs. Once the coatings corrode seriously, the fraction and wear properties are also decreased straightly. Therefore, the application of WC-10Co-4Cr coatings in the complex environment still needs to investigate. Rare earth elements (REEs) are widely used in modifying the coatings due to the especial electronic structure. Several studies on the effect of REEs on the corrosion and wear resistance for WC/Co(Cr) coatings has been carried out. However, the mechanism of REEs on the properties of coatings is still obscured. Based on those, the nanoadditives (containing REEs) modified WC-10Co-4Cr coatings were prepared by HOVF. The micro hardness, fraction and wear properties were investigated to reveal the mechanism of nano-additives on the fraction and wear properties of WC-10Co-4Cr coatings.

The hardness tests showed that the micro hardness increases with the increasing nanoadditives content, which is attributed to the restrained effect of nano-additives on the decarburization of WC. Moreover, the addition of nano-additives is always segregated at the grain and the phase boundaries, which increases the melting of WC particles and thereby restraining the growth of grains. Meanwhile, the nano-additives is adapted to react with the impurities at the grain boundaries to form stabilized compounds, which is also factor of increasing the micro hardness. Besides, the decreased pores with the increasing nanoadditives content are essential effects on the micro hardness.

The abrasion loss of nano-additives modified WC-10Co-4Cr coatings is obviously lower than that of WC-10Co-4Cr coating without adding nano-additives. And the abrasion loss is decreased with the increasing nano-additives content. The friction coefficient showed two-step characteristics. At the first stage, the friction coefficient increases with time which is related to the rough surface of friction pair. After that, the friction coefficient trends to steady. As a whole, the addition of nano-additives into the WC-10Co-4Cr coatings decreases the friction coefficient, which is due to the promoted microstructure and phase component of WC-10Co-4Cr coatings. The addition of nano-additives decreases the pores in the coatings and restrains the decarburization of WC, and subsequently the nanoadditives modified WC-10Co-4Cr coatings is so compact that plays a key role in promoting the friction and wear properties.

The worn surface morphology of WC-10Co-4Cr coating without nano-additives displayed the lamellar characteristics, which implies that plastic deformation and fatigue rupture occur during the wearing process and further resulting in the layer-by-layer spallation. Adding 3% nano-additives into the coatings decreases the lamellar amount, which implies the friction and wear properties are promoted. It is also confirmed that the phase components of both coatings are different. Both of them are consisted of the coatings themselves and Fe-oxide which is caused by the high temperature oxidation of 40Cr friction pair during the wearing process. According to the area of coatings themselves, it can be estimated that the abrasion loss of coating without nano-additives is much more than that with nano-additives. Then the wear crack of coating without nano-additives is so deeper than that with nano-additives. Above-mentions indicate that the addition of nanoadditives promotes the friction and wear properties of WC-10Co-4Cr coatings.

Keywords: thermal spraying, WC-10Co-4Cr, nano-additive, tribological property

Wear behaviors of the arc-sprayed FePSiB-based amorphous and nanocrystalline coatings

Jiangbo Cheng¹, Qin Zhang², Dan Liu², Yuan Feng², Xiubing Liang³

(1. Hohai University; 2. College of Mechanics and Materials, Hohai University;

3. National Institute of Defense Technology Innovation, Academy of Military Sciences PLA China)

chengjiangbo@hotmail.com, liangxb_d@163.com

Abstract: The aim of this paper was to investigate the effects of Cr and Nb additions on the microstructure and wear behaviors of the FeSiBP coatings. The FeSiBP-based cored wires containing low purity industrial raw materials with high glass formation ability were adopted as the precursor reactants. A series of the FeSiBP-based coatings were in situ synthesized by using arc spraying process. The microstructure of the coatings was characterized by SEM, XRD, and TEM. The microstructure of the FeSiBP coating consists of nanoscale α Fe phase. With addition of the Cr and Nb, the average size of the nanoscale particles is reducing and a full amorphous phase is identified in the FeSiBPCrNb coating. The formation mechanisms of the amorphous phase and nanocrystalline were discussed in details. The dry sliding wear behaviors and mechanisms of the FePSiB-based amorphous/nanocrystalline coatings were investigated in reciprocating mode against a WC counterface with different sliding speeds and normal loads. The wear rates of the FePSiB-based coating are increasing linearly as a function of the normal loads and sliding speeds. The addition of Cr and Nb brings about a significant improvement in the friction and wear behavior of the FePSiB coating. When the normal load is 60 N and sliding speed is 45 mm⁻¹, The relatively wear resistance of the Fe65P5Si9B10Cr10Nb1 coating is about 3.8 and 6.2 times that of the Fe65P5Si9B10Cr10 coating and the Fe65P5Si9B10 coating, respectively. The analysis of worn morphologies shows that an increase in normal load and sliding speed creates an oxidative tribo-film. The coverage region, thickness and stability of the oxide tribo-films on the worn surface of the coatings are increasing with the additions of Cr and Nb under the same dry sliding wear conditions. The successive and compact oxide tribo-film is beneficial to the wear resistance of the coating. The dominating wear mechanisms of the FePSiB-based coatings are combination of abrasion and delamination failure coupled with oxide wear. Nano-mechanical characterization was done to map the correlation between the evolutions of elastic properties and the wear resistance of the coatings. The excellent wear resistance of the Fe65P5Si9B10Cr10Nb1 coating is attributed to its finer nanoscale grain and a full amorphous phase concurrent structure, the better elastic recovery properties and the formation of compact oxidative tribo-films on the worn surface. The FePSiB-based amorphous and nanocrystalline coatings prepared by low cost arc spraying process with combination of high GFA and superior mechanical properties, provides valuable guidance for expanding engineering applications.

Keywords: sliding wear, coatings, thermal spraying process

Influence of grit dimension on the friction and wear behavior of CT80 tubing

Hui Dong
(Xi'an Shiyou University)
donghuihy@163.com

Abstract: The crude oil still contains some different dimensional grit grains although grit control net filter is employed. The durability of oil well pipe is dramatically decreased because of the wear induced by grit grains. Meanwhile, the size of grit grain is also a factor that influenced the durability and wear mechanism of oil well pipes. Unfortunately, how the size of grit grain affects the friction and wear behavior of oil well pipes is still not clear yet. The tubing named CT80 was selected as an example to evaluate how the grit grain size affects the oil well pipes in production of crude oil. The other friction pair was a high strength cable. The dimensions of tubing specimens were all 70 mm×70 mm×4.6 mm. The cable specimens were curved cylindrical specimens. The tubing and cable were all immersed in the crude oil during friction test. The sizes of grit grains are 100, 200, 300, 400 and 500 μm, respectively. To understand the variation of wear behavior caused by grit grain size, the other factors such as wear speed, loading and content of grit grain were fitted, which were 0.7 m/s, 100 N, and 8%, respectively. The wear duration was 8 h. The friction coefficient was recorded during wear test. The thickness reduction and the wear rate of the tubing was calculated through the weight loss and the wear area. To analyze the friction and wear behavior, the morphology characteristics of the worn surfaces as well as the cross-sectional were observed via a scanning electron microscope (SEM) and a metallographic microscope. Induced elements transformation in test has been detected by using an energy dispersive spectrometer (EDS). The results show that when the grit size increases from 100μm to 300μm, the weight loss and wear rate of the tubing increases slowly. It means that the grit grain size contributes little to wear rate of tubing when it size is lower than 300 μm. However, the weight loss and wear rate dramatically increases when grit grain size increases from 300 μm to 400 μm. Then, the weight loss and wear rate decrease as grit grain size increases. It indicates that there is a critical size of grit grain, corresponding to the most serious wear of tubing. The change rule of friction coefficient is nearly identical with that of weight loss. Thus, the grit grain size indeed affects the wear behavior of tubing, mainly depending on the friction coefficient. The wear mechanism of the tubing in the case is mainly abrasive wear, accompanying with a little corrosion wear, when the grit grain size is less than 400 μm. When the grit grain size reaches 400 μm, ratio of the corrosion wear increases significantly. Thus, the wear mechanism transfers into abrasive wear and corrosion wear, once the grit grain size reaches 400 μm. The wear is mainly controlled by the corrosion when grit grain size exceeds 500 μm. As a result, the wear rate decreases. With increasing of grit grain size, the residual anti-displacement strength and the remaining anti-inner pressure strength of the tubing decrease first and then increase. When the grit grain size is 400 μm, the minimum residual anti-displacement strength and remaining anti-inner pressure strength are 60.35 MPa and 63.07 MPa, respectively.

Keywords: CT80 tubing, grit dimension, wear mechanism, residual strength

Friction and wear behavior of H13 steel processed by laser surface remelting

Zhixin Jia¹, Yitao Yu¹, Jiqiang Li¹, LiJun Liu¹, Honglin Li²

(1. Ningbo Institute of Technology, Zhejiang University; 2. Ningbo University)

jzx@nit.zju.edu.cn

Abstract: AISI H13 steel is the most commonly used hot work tool steel for die casting dies. Friction, wear behavior and thermal fatigue properties are important factors which influence the service life of dies. In this paper, quenched and tempered AISI H13 tool steel was selected as the substrate. Specimens with different laser track spacings were processed by laser surface remelting using an Nd:YAG laser and were prepared to study the friction and wear behavior at 300 °C. YG15, a kind of cemented carbide which can be used as cutting tool, was selected to be the counterpart to carry out the friction and wear test.

Specimens with different laser track spacings and the counterpart are heated to 300 °C by a heating furnace during the friction and wear test. The specimen rotates at 100 r/min and the counterpart remains static with a contact pressure force of 70 N. Each duration of a complete friction and wear cycle was 6 hours. After 6 hours the specimen and counterpart are cleaned and dried. The weight loss of the specimen is measured with the FA2004 current analytical balance and the average weight loss of the three specimens was recorded. In order to investigate the effect of laser tracks on wear resistance, scanning electron microscope (SEM), X-ray diffraction (XRD), energy dispersive spectrometer (EDS) and 3D profilometer were used. The microstructure, microhardness, mass loss, friction coefficient, and wear mechanism are discussed.

The microstructure and microhardness of the laser remelted area were analyzed. The microstructure of the laser remelted zone is composed of more fine grains than that of the H13 substrate. The microhardness of the laser remelting zone is about 135 HV higher than the H13 substrate. After friction and wear test, the microhardness of both the laser remelted zone and substrate decrease slightly, and microhardness of laser remelted zone remains higher than that of the substrate.

The results of dry sliding wear tests indicated that the wear resistance of specimens processed by laser remelting has a remarkable improvement in comparison to the untreated specimen. The improvement in wear resistance at high temperature is directly related to the ratio of the laser remelted area. During the wear process, the finish of the laser remelted tracks is better than that of the H13 substrate. The friction coefficient of the specimen also increases with the ratio of the laser remelted area. The wear resistance increase and the mass loss drops with the increasing of laser remelting surface ratio.

Keywords: friction and wear behavior, laser surface remelting, H13 steel, microstructure

Comparative study on microstructures and tribological properties of the sulfurizing layers prepared on different cladding coatings

Gang Cui, Bina Han

(College of Mechanical and Electronic Engineering, China University of Petroleum, Qingdao, China)

cuingang_1989@126.com

Abstract: To determine the influence of the sulfurized substrate on the compositions and tribological properties of the ion sulfurizing layers, the low temperature ion sulfurizing technique was carried out on Fe, Ni and Co based laser cladding coatings in this paper. The microstructures of the laser cladding/ion sulfurizing layer (sulfurizing composite layers) were investigated by SEM, EDS, AFM and XRD. The results implied that the sulfides solid lubricant films were successfully fabricated on surface of the laser cladding coatings. The FeS phase was detected in the three kinds of sulfurizing composite layers and the WS₂ phase was detected in the sulfurizing layers prepared on Ni and Co based cladding coatings because of the addition of WC particles in the cladding powders.

The tribological properties were investigated by pin-on-disc tester. The experimental results showed that the friction coefficients and wear losses of the sulfurizing composite layers decreased apparently in contrast to the cladding coatings without being sulfurized, and the tribological properties of the three kinds of sulfurizing composite layers were improved differently. The sulfides solid lubricant film on Co based cladding coatings showed best anti-friction performance. In addition, to test the influence of the sliding speed and load on the performance of the lubricant films, the tests were run at the sliding speeds ranging from 0.1 m/s to 1.2 m/s, the load ranging from 10 N to 80 N. It showed that the tribological properties of the sulfides film on different coatings performed the similar tendency as the speeds and loads increased. And the sulfides film on Co based coatings performed best at higher speed and load than the others. The morphologies and the phase compositions of the worn surface were analyzed by SEM, EDS, AES and XPS, the results showed that the adhesive wear and abrasive wear were main wear mechanisms and the oxidations and the corrosions were both generated during the rubbing. Finally, according to the results obtained by the sulfides films and the cladding coatings, the mechanism of anti-friction wear was analyzed and discussed. From the mechanism discussed in the paper, it indicated that the sulfurized substrate with higher hardness and corrosion resistance could help the sulfides solid lubricants show lower friction coefficient and work longer.

Keywords: ion sulfurization, laser cladding coatings, sulfur formations, tribological properties

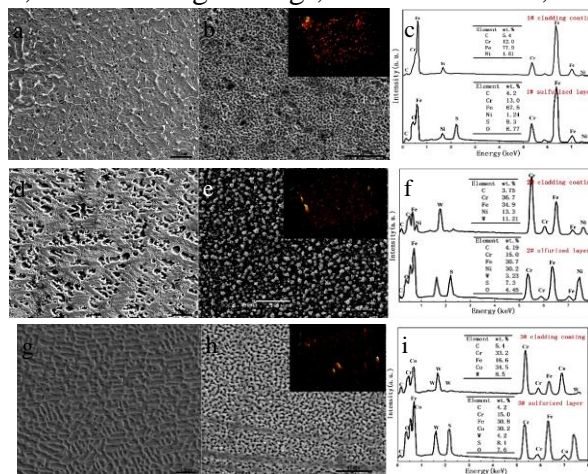


Fig.1 Surface morphologies and EDS results: (a) Fe-based coatings; (b) Fe-based sulfurizing composite coatings; (c) EDS results of Fe-based coating and sulfurized layer; (d) Ni-based coatings; (e) Ni-based sulfurizing composite coatings; (f) EDS results of Ni-based coating and sulfurized layer; (g) Co-based coatings; (h) Co-based sulfurizing

Abrasive wear of an advanced medium Mn transformation induced plasticity steel

Xiaojun Xu, Qibin Tang, Yiwen Hu, Minhao Zhu
(Southwest Jiao Tong University)
xiaojunxu0617@126.com

Abstract: Medium-Mn steels having superior combinations of high strength and good ductility, a good strain hardening capability, as well as affordability, represent a very successful engineering steel family for automobile and other structural applications. The outstanding mechanical properties offer a great potential for the development of high abrasion resistant steel, especially strengthening by strain (abrasion)-induced martensitic transformation (TRIP effect) during abrasion process. However, the current studies on medium-Mn steels mostly focus on their mechanical tensile properties, while the abrasive wear has been studied much less. This paper will systematically investigate the abrasive wear behavior of a medium-Mn steel. Of importance is to unravel the mechanism of stress (abrasion)-induced martensitic transformation and its effect on the reinforcement of abrasion resistance. The results suggest that strain-induced martensitic transformation has a significant influence in determining the abrasion resistance and that the effect is contact load dependent. Moreover, the dynamic process of microstructure evolutions during abrasion process and the abrasive wear mechanism under the different loading condition have been analyzed.

Keywords: abrasion resistance, medium-Mn steel, strain-induced martensitic transformation, microstructure, abrasive wear mechanism

Surface microstructure evolution of CL65 in wear

Rui Pan, Ruiming Ren, Chunhuan Chen, Xiujuan Zhao
(Dalian Jiaotong University)
rmren@djtu.edu.cn

Abstract: During the operation of the wheel-rail, the surface of wear will form significant plastic deformation layer and even appear white etching layer, leading to wheel-rail contact surface failure, such as contact fatigue, spalling or even polygonization wear. Therefore, studying the surface microstructure evolution of wheel-rail materials in the process of wear is great significance for improving the life of wheel-rail. In this paper, rolling and sliding wear tests were performed on CL65 wheel steel to study the evolution of surface structure during wear. The results showed that the pearlite on the surface underwent through the following plastic deformation: the direction of pearlite lamellae gradually tended to become parallel to that of the wear surface and the spacing between pearlite lamellae also became smaller during rolling wear due to the impacts of compressive stress and shear stress. When the spacing was less than 100nm, most of cementite began to fracture and dissolve and the ferrite inside the pearlite displayed the feature of subgrains refinement because of plastic deformation. Eventually, the bar-shaped ferrites with certain preferential orientation were formed and the undissolved, fine and small cementites were scattered in the vicinity of their boundaries. Inside hypoeutectoid steel, pro-eutectoid ferrite with low hardness would undergo subgrains refinement due to plastic deformation; some subgrain boundaries were gradually transformed into large-angle boundaries, leading to ferrite refinement. During sliding wear, the bar-shaped ferrite was refined into subgrains, through accumulation of dislocations caused by further plastic deformation with the further enlargement of strain. Then, the nanometer-sized level ferrite grains with random orientation were formed.

Keywords: wheel steel, microstructural evolution, rolling wear, sliding wear

A wear trend forecasting model of gas turbine ongoing research based on optimized genetic algorithm and improved bp neural network

Jiasi Sun, Hong Lang, Yujia Liu, Zhenyu Han
(AECC Shenyang Engine Research Institute)
jessieaprilsun@163.com

Abstract: An appropriate approach combined genetic algorithm (GA) and improved BP neural network (BPANN) was proposed for wear trend forecasting of the oil-lubricated system of a certain gas turbine engine independently designed by our institute during 500 h test. Based on the oil spectral analysis data of the classic metal element, the combinational model with the modification of the learning rate and the optimization of the initial weights and thresholds by GA was carried out to accelerate the convergence speed of the standard BPANN and avoid being trapped in local minima. Also, real coding was adopted in the encoding process of GA to enhance forecasting efficiency and exert maximum performance of the model. As a result, compared with the standard BPANN the combinational model has obtained more ideal solutions for wear trend prediction of lubricating system, and its wear prediagnosis result is in accord with the actual disassembly examination after the test.

Keywords: wear trend forecasting, gas turbine ongoing research, oil-lubricated system, bp neural network, genetic algorithm

Tribological properties of plasma sprayed Al₂O₃-TiO₂ coatings with nano graphite

Yue Wang¹, Saiyue Liu¹, Junfeng Gou¹, Qiwen Zhang¹, Dongxia Zhen¹, You Wang¹, Ruiqing Chu²
(1. Harbin Institute of Technology; 2. Yantai University)
wangyou@hit.edu.cn

Abstract: In this paper, different contents of nano graphite were added into the nano-structured Al₂O₃-TiO₂ sprayable feedstocks by ball-milling process. The Al₂O₃-TiO₂ coatings with or without nano graphite were fabricated by plasma spray technology using sprayable feedstocks. Then, the effect of nano graphite on tribological properties of Al₂O₃-TiO₂ coatings was studied by performing dry sliding wear testings under normal loads of 5, 10 and 15 N. Surface morphologies of coatings before and after wear testing were observed by SEM. Finally, wear mechanism of the coatings was discussed.

The results showed that nano graphite could improve the tribological properties of coatings. The friction coefficient decreased with the addition of nano graphite from 0% to 12% under different normal loads. Nano graphite decreased the wear rate of coatings remarkably. The content of carbon (C) on the worn surfaces of coatings with nano graphite was larger than that without nano graphite, indicating that graphite was adhered on the worn surfaces during the wear process. The adhered graphite acting as lubricant could separate coatings and the counter balls efficient, which played a role of reducing the degree of adhesion during the sliding wear testing.

Keywords: plasma spraying, nano-structure, Al₂O₃-TiO₂, tribological properties, nano graphite

Study on strengthening wear resistance and friction reducing of epoxy composite coatings

Yan Hao, Xiying Zhou
(Shanghai University of Engineering Science)
zhouxiying@sues.edu.cn

Abstract: To strengthen the friction-reducing and wear-resistance performance of epoxy resin composite coatings, this work uses hard particles of silicon carbide, diamond and solid lubricant graphite, molybdenum for filling and modification, which aims at reducing the surface friction coefficient and wear volume of the composite coatings through synergy between the fillers. The surface morphology of the wear surface, wear debris and phase composition were observed and analyzed by means of scanning electron microscope, energy spectrometer and X-ray after friction wear test. The results show that the synergistic effect between the fillers can improve the tribological properties of the material. The wear mechanism of epoxy resin composite coating is mainly abrasive wear and fatigue wear. Compared with the epoxy resin, the friction coefficient and the wear volume of the modified composite coatings were respectively reduced by 17.24% and 42.57%.

Keywords: epoxy resin, composite coating, wear-resistant, friction-reducing

Finite element analysis of non-linear contact wear of

U-shaped ring of power tools

Pingping Lu, Xinmei Li
(School of Mechanical Engineering, XinJiang University)

Abstract: With the increase of running time, our country has been built in the northwest region UHV transmission lines, line hardware appeared different degree of wear and tear. Especially in wind region of transmission line, because suffered wind larger more frequent, severe wear degree than other areas. So this paper is established U-shaped ring wear model by finite element software, and analysis, in ANSYS Workbench, U-shaped ring in 0.8 T (8000 N) under the action of load, the wind cause U ring in different Angle (0-30 °) stress variation, and the analysis of u-shaped ring in different load 0.4 T, 0.6 T, 0.8 T (4000 N, 6000 N, 8000 N), different wear cycles (5 w, 10 w, 15 w) under the action of the boundary conditions of wear size. Finally by comparison with experimental value and simulation value analysis can be concluded that the finite element model of the friction and wear can better simulate the U-shaped ring wear, simulation results and experimental results have the same change trend, the overall simulation results with the test results on the whole there is always a small fluctuations, but the rest after the finite element simulation of wear size close. The test results as in a strong wind area of the transmission line hardware provides the theory basis for design, overhaul and maintenance.

Keywords: transmission line, U-shaped ring, ANSYS Workbench. Stress, Angle, Wear and tear

Sliding wear behavior of nano-structured Al₂O₃-YSZ coatings

fabricated by plasma spraying

Zhaoyi Pan¹, Yifeng Xu¹, Guoxin Song¹, You Wang²

(1. Xi'an Space Engine Company Limited;

2. Department of Materials Science, Harbin Institute of Technology)

pan_zhaoyi@126.com, wangyou@hit.edu.cn

Abstract: This paper reports studies into the sliding wear behavior of Al₂O₃-20wt% YSZ (ZrO₂ + 8wt% Y₂O₃) coatings fabricated by plasma spray. The effect of plasma treating to feedstocks on wear resistance of coatings was researched. The sliding wear tests were carried out using a pin-on-disk wear tester against with GCr15 and ZrO₂ balls at different normal load. The results indicate that the friction coefficient and wear rate of coatings wore against with GCr15 are much lower than that of coatings against with ZrO₂. The wear mechanism of coatings wore against with GCr15 was adhesive wear and oxidation wear with adhesive transferences and ferric oxide film. The ferric oxide film can increase the wear resistance of coatings, with mild fracture of micro-peaks on the rough worn surface. By analysis of worn surface profile, the wear rate is about $1.1902 \times 10^{-3} \text{ mm}^3/(\text{N m})$ for coatings fabricated from heat treated feedstocks, and it is only $1.1039 \times 10^{-4} \text{ mm}^3/(\text{N m})$ for coatings fabricated from plasma treated feedstocks. The damage of the coatings after sliding wear against with ZrO₂ was brittle fracture and spallation of splats caused by cracks intersection. The technology of plasma treating to feedstocks is beneficial to increase the wear resistance of coatings.

Keywords: thermal spray coatings, sliding wear, surface analysis, wear testing, contact mechanics

Friction and wear properties of argon arc cladding Ni-based

nanocrystalline coatings

Junsheng Meng, Mingyu Wang, Xiaoping Shi

(1. College of Naval Architecture & Marine Engineering, Shandong Jiao Tong University

Weihai Campus, Weihai 264209, China)

mengjs2008@163.com

Abstract: The TiN-TiB₂ nanocrystalline cladding layers were in-situ synthesized on the surface of 35CrMnSi steel using argon arc cladding technology. The effects of (Ti+BN) content on the microstructure, micro-hardness, friction and wear properties of argon arc cladding Ni-based coating were investigated by XRD, SEM, TEM, micro-hardness tester, friction and wear tester. The results showed that, the main phase composition of the cladding layers is TiN, TiB, TiB₂, Cr₂₃C₆ and γ -Ni. Compared with Ni60 cladding layer without TiN-TiB₂ nanocrystalline, the micro-morphology of Ni-based nanocrystalline cladding layers respectively are preferable, which are smoother and without obvious pores and cracks. The microscopic structure of the cladding layers mainly consisted of granular, needle and rod-like. The micro-hardness of the cladding layers from the surface to the substrate is gradually decreased with increasing depth of the cladding layer. The cladding layers micro-hardness still increase with the increase of (Ti+BN) content. The tribological behavior of both the substrate and the cladding layers was investigated in detail. As the (Ti+BN) content about 30% percent, the coating showed not only compact structure, but also good wear resistance at the room temperature under normal atmosphere conditions.

Keywords: argon arc cladding, nanocrystalline, microstructure, friction and wear properties

Influences of yttrium addition on the porosity reduction and tribological properties of (W, V, Ti)C-8%Co cemented carbide alloy

Linbo Chen, Guomin Hua
(Jiangsu University)
guomin@ujs.edu.cn

Abstract: In comparison with the traditional WC-Co cemented carbide alloy, solid solution cemented carbide alloy, such as (W, Ti, V)C-Co, has received considerable attention due to the remarkable performances on strengthening by grain refinement and resisting chemical attack, diffusion wear during steel cutting. However, the (W, Ti, V)C-Co cemented carbide alloy was suffered from the porosity during the sintering process, which arose from poor wettability between VC and Co binder. In this study, attempt will be made by combining first-principles calculation and experiments to investigate the influence of yttrium addition on porosity reduction and tribological properties of (W, Ti, V)C-Co cemented carbide alloy. and corresponding mechanisms will be discussed in detail.

Keywords: cemented carbide alloy, tribology, first-principles calculation

Influence of the cementite morphology on rolling wear of D2 wheel steel

Lin Ma, Pengtao Liu, Jinzhi Pan, Ruiming Ren
(School of Materials Science and Engineering)
rmren@djtu.edu.cn

Abstract: In this experiment, rolling wear tests were performed on D2 wheel steels which have different original microstructures, the cementite morphologies of which are granular (G-Cem) and lamellar (L-Cem). Using electronic scales, OM, SEM and Vickers hardness tester to analyze the samples after tests to study the influence of the cementite morphology on rolling wear of D2 wheel steel. The results showed that in the process of rolling wear, the surface damage morphology of G-Cem was dominated by adhesive wear, while for L-Cem, it was dominated by fatigue wear. With the increase of the wear cycles, the degree of hardening was both greater. Meanwhile, the thickness of the plastic deformation layer of the G-Cem was larger. However, the wear resistance of G-Cem was worse. The reason was that during rolling wear, due to the vertical mechanical vibration, G-Cem was more likely to form polygonization wear that causing more mass loss, which would accelerate the failure of the samples.

Keywords: wheel steel, granular cementite, lamellar cementite, rolling wear

Research on friction and wear properties of quenching partitioning-tempering steel

Tingwei Zhang, Zhen Zeng, Jilan Yang, Zhenghong Guo, Jianfeng Gu
(Institute of Materials Modification and Modelling, School of Materials Science and Engineering,
Shanghai Jiao Tong University, Shanghai 200240, China)
siriuswater@sjtu.edu.cn

Abstract: The quenching and partitioning (Q-P) steel has been proposed to improve ductility of martensitic steels due to the effect of transformation-induced plasticity by retained austenite. The Q-P process contains a full or partial austenitization followed by a fast quenching to martensite transformation and an isothermal partitioning step. During the partitioning procedure, the carbon atoms in supersaturated martensite partition to neighbor austenite, which leads to the carbon enriched retained austenite with higher mechanical stability. In this kind of steel, the microstructure contains martensitic matrix and considerable amount of retained austenite, of which the former is responsible for the high strength and the later contributes to excellent plasticity. In order to further improve the strength and plasticity of this steel, Xu has proposed to add some alloy elements to form carbides precipitation in the martensitic matrix due to its precipitation strengthening effect, that is quenching-partitioning-tempering (Q-P-T) steel. Because of its good comprehensive mechanical property in addition to the low cost, many scholars and enterprises have paid much attention to develop suitable processing parameter and optimized compositions for industrial manufacturing, while the potential failure risk of Q-P-T component after service including the wear property has not been concerned sufficiently. Therefore, the dry sliding friction and wear properties of Q-P-T steel were studied in this paper. The factors affecting wear resistance, including the content of retained austenite and its stability, and the working conditions of contact load and sliding velocity, were investigated. In addition, selecting the Q&P steel with identical chemical element as reference, the influence of the carbide precipitation was analyzed as well. The results show that the microstructure of the Q-P-T steel is composed of the lath martensite and the retained austenite, with carbide particles dispersed in the martensitic matrix by transmission electron microscopy (TEM) and electron backscatter diffraction (EBSD) analysis. The contact load and sliding velocity have a great influence on the wear resistance. The wear morphology observation was found out that, with the increase of the contact load, the wear feature changed from the microploughing to the adhesive manner. However, at very high load level, due to the low stability of retained austenite caused by low carbon concentration, martensitic transformation may occur in the process of friction, not only leading to the local hardening of the surface, but also contributing to the additional compressive stress caused by the volume expansion. This is beneficial to the better wear resistance; In addition, it is true that the distribution and size of carbides have different influences on the wear resistance of the Q-P-T steel.

Keywords: quenching-partitioning-tempering steel, dry sliding friction and wear, retained austenite, martensitic transformation, carbides

Effect of cryogenic treatment on mechanical properties and microstructure of

42CrMo after thermo-mechanical processing

Haidong Zhang¹, Xianguo Yan¹, Shenggang Feng²
(1. Taiyuan University of Science and Technology;
2. Dingxiang Baoguang Steel Products Manufacturing Co., Ltd.)
yan_xg2008@126.com

Abstract: The Conical pick is a widely used cutting tool in roadheaders in mining industry, which is made by inserting and welding a cemented carbide tip to a steel pick body. During the cutting process of the conical pick, the wear or fracture of the pick body occasionally occurs which lead to the failure of the conical pick. Therefore, improving the mechanical properties of the pick body can be an important way to increase the service life of the pick.

The cryogenic treatment is an extension of conventional heat treatment of heating-quenching-tempering cycle and typically carried out between quenching and tempering, which has been practiced on steels and tungsten carbides to obtain significant improvement of hardness, toughness, wear resistance or to relieve residual stress.

In this research work, the raw material of 42CrMo, a widely used materials for making pick bodies in China's mining industry underwent a thermo-mechanically processing, which is a combination processing of forging and quenching, then different cryogenic treatments were applied to the material ,in the end tempering was carried out at 250 °C for 2.5 hours. Taguchi design method, a fractional factorial design based on a orthogonal arrays proposed by Dr. Genichi Taguchi, greatly reducing costs and time of experiments was employed to conduct the cryogenic treatment experiment to investigate the effect of different parameters of cryogenic treatment, namely soaking temperature (-80, -120, -160, -196 °C), soaking time (4, 8, 12, 24 hours) and treatment cycles (1, 2, 3, 4 cycles) on mechanical properties of the specimens such as hardness, impact toughness and wear resistance.

Rockwell hardness testing, Charpy impact toughness testing and pin-on-disk wear testing were carried out to measure the hardness, impact toughness, wear resistance of the specimens respectively after above processings.

The microstructure and fractography of the specimens after impact testing and the microstructure and surface topography of the specimens after wear testing were observed by scanning electronic microscope (SEM). Phases in specimens were observed by X-ray diffractometer (XRD) to analyze the phase transformation before and after cryogenic treatment.

The experiment results show that the cryogenic treatment has a significant influence on mechanical properties of the 42CrMo material and the factor of soaking temperature has the largest impact on mechanical properties of the 42CrMo material whereas the factors of soaking time and treatment cycles have less impact on mechanical properties of the 42CrMo material.

Specifically, after the cryogenic treatment hardness slightly increased and increased more at lower soaking temperature, but the impact toughness mostly decreased, and decreased more slowly at lower soaking temperature. And after the cryogenic treatment the wear resistance improved significantly and the lower the soaking temperature, the better the improving.

By analyzing the results of SEM and XRD before and after cryogenic treatment of the material, it can be concluded that the cryogenic treatment can promote the martensitic transformation of retained austenite and refinement and precipitation of carbides of chromium, which contribute to the improvement of the wear resistance of the material.

Keywords: cryogenic treatment, taguchi design method, wear resistance

Study on dry sliding friction-induced deformation layers at different wear stages of 30CrMnSi steel and its wear behavior

Peng Zhu¹, Shuang Liang¹, Jidong Zhu¹, Yudan Yang¹, Xing He¹, Wurong Wang¹, Xicheng Wei¹
(1. School of Materials Science and Engineering, Shanghai University, Shanghai 200444, China;
2. Zhejiang Jiajie Plastic Co., Ltd, Yiwu 322000, China)
zp19940502@163.com

Abstract: Plastic deformation and damage accumulation in friction-induced deformation layers directly affect the friction behavior of a tribo-system. The present studies have primarily focused on the friction wear-induced structural evolution of austenitic stainless steels, rail steels or single-phase material, such as titanium and pure copper at a certain wear stage. However, most studies have not systemically analyzed the correlation between wear behavior and evolution of microstructure and mechanical properties in subsurface during the whole wear process, especially the role of strain-hardening induced by plastic deformation in deformation layers, which accordingly alters the wear behavior.

In the present work, dry sliding friction and wear behaviors of the normalized 30CrMnSi steel against quenched and tempered GCr15 steel were studied using a pin-on-disc tester. The wear behavior and plastic deformation of the friction-induced deformation layers at different wear stages were investigated ensued. Test was carried out at room temperature with the normal load of 100 N, sliding speed of 0.52 m/s and the duration of sliding wear was 15, 60 and 240 min respectively. The microhardness of normalized 30CrMnSi steel pin was 220 HV while that of GCr15 steel disc was 60 HRC. The worn surface morphology and subsurface structure of different sliding time was analyzed using scanning electron microscopy (SEM). The hardness of cross section was obtained by Vickers microhardness testing machine with a load of 10 gf for 15 s.

It was found that the wear rate drops with the increasing sliding time and three wear stages could be divided based on the variation of wear rate: rapid wear, slow wear and stable wear (Fig.1). The SEM morphologies of the worn surfaces suggested their main wear mechanism were adhesive and abrasive. With the extension of sliding time, the surface oxidation was more serious and large debris owing to the worn surface exfoliation gradually decreased so that wear loss relatively diminished. The thicknesses of the plastic deformation zones were in the range of 55-85 μm . The affected depth tended to decrease when the wear rate increased and kept relatively constant at stable wear stage. The closer to the worn surface, the severer deformation of microstructure was. During the stage of rapid wear (Fig.2a), the lamellar pearlite was broken and dropped from matrix, then cracks and holes were formed resulting in the appearance of large debris. The refined structure was formed by the rapid accumulation of strain and the increase of dislocation with the prolongation of sliding wear duration (Fig.2b, 2c).

The estimated maximum equivalent strain beneath the worn surface after test for 240 min was about 5.15, which is similarly twice as much as that after test for 15 min (Fig.3). This obviously shows that the pin in 240 min undergone severer plastic deformation than that in 15 min at the same depth. The equivalent strains of deformation layers for 30CrMnSi steel decreased as the depth from worn surface increased.

Compared with the matrix, the hardness near the worn surface of the pin (Fig.4) was strikingly increased as a result of cumulative strains and a large strain gradient which occurred in subsurface. The microhardness decreases with increasing depth which is in accord with the variation tendency of shear strain and finally the microhardness remains constant at 220 HV at different depths.

Results illustrate the correlation between the wear behavior and plastic deformation in friction-induced deformation layers, and reveal that during the sliding wear process, a competition between the phenomenon of strain-hardening and the wear: the unceasing removal of matter due to the abrasion indeed restrict the deepening of the strain-hardening layer.

Keywords: dry sliding friction, plastic deformation, strain-hardening, wear behavior

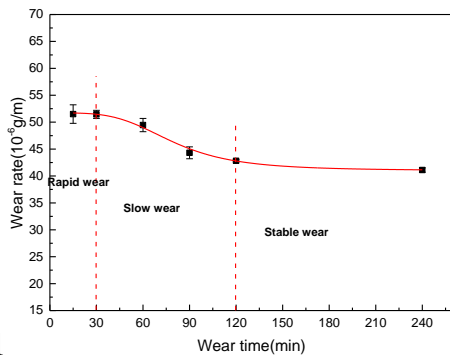


Fig.1

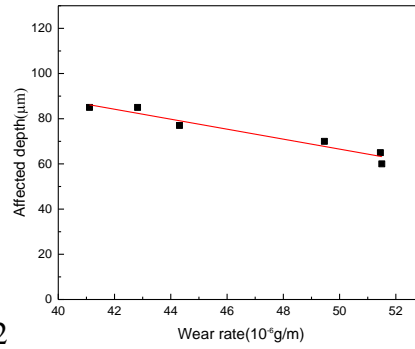


Fig.2

Fig.1 Variation curve of 30CrMnSi steel pin wear rate

Fig.2 Affected depth versus the wear rate

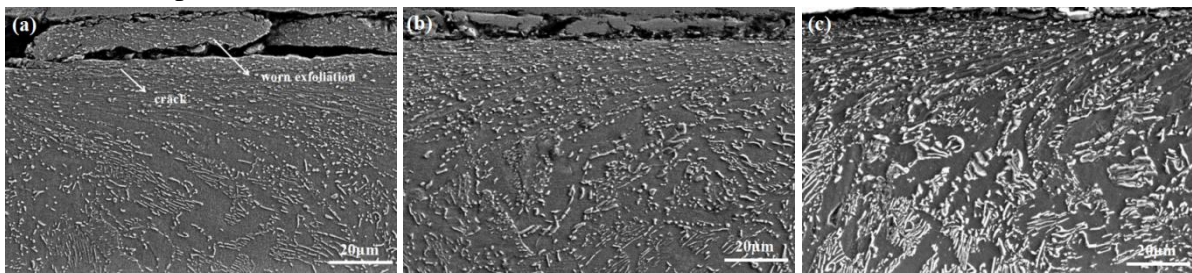


Fig.3 Cross-sectional microstructure of 30CrMnSi steel pin during different sliding time: (a)15 min; (b) 60 min; (c) 240 min

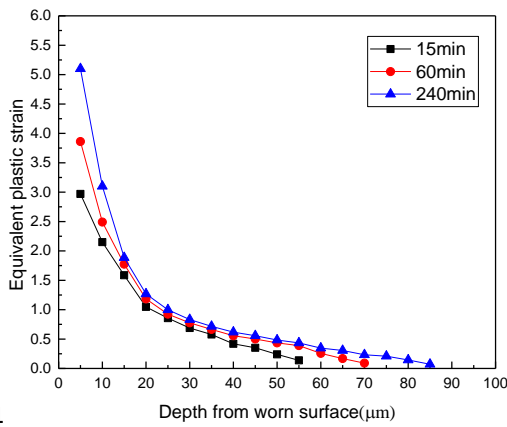


Fig.4

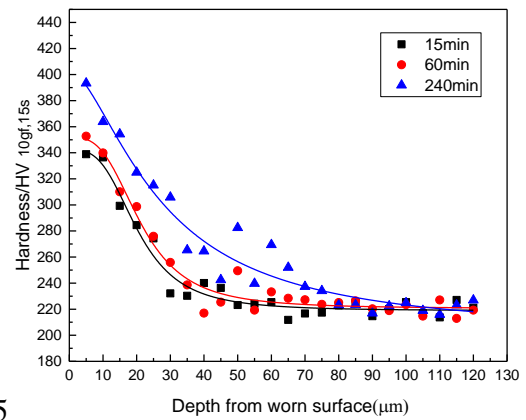


Fig.5

Fig.4 Estimated equivalent strain at different depths

Fig.5 Microhardness gradient from worn surface to interior

Microstructure and tribological properties of micro-arc oxidation TiO₂ coating before and after SiC particles incorporation

Limei Ren, Tengchao Wang, Zhaoxiang Chen, Xipeng Ren
(Yanshan University)
zxchen@ysu.edu.cn

Abstract: The porous TiO₂ ceramic coating was fabricated on the surface of commercially pure titanium using the micro-arc oxidation (MAO) technique. However, this fabrication process usually results in high porosity and surface roughness of the MAO coating which causes a high friction coefficient and low wear resistance under non-lubrication conditions. In order to improve the tribological performance of MAO TiO₂ coatings, researchers dispersed functional particles in the MAO electrolyte and attempted to incorporate these particles into the MAO TiO₂ coating during the anodization process. Therefore, the purpose of this work is to obtain micro arc oxidation composite ceramic coating with good friction and wear properties by incorporating SiC sub-micron particles on the surface of commercial pure titanium (TA2). A commercially pure titanium plate, with a size of 25 mm×80 mm×1 mm, was used as the substrate for fabricating MAO TiO₂ ceramic coating. Prior to MAO processing, all samples were polished with 180, 400, 800 and 1500# SiC sandpapers, then washed with 95% alcohol by ultrasonic cleaning. Finally, all samples were cleaned with distilled water and dried in warm air. The electrolyte consisted of Na₂SiO₃ (15 g/L), Na₃PO₄ (10 g/L), NaOH (1 g/L), and the concentrations of SiC particles was 0, 4 and 12 g/L, respectively. A pulsed asymmetric bipolar AC power supply was employed to fabricate ceramic composite coatings on the titanium surface. And the anodization of titanium was carried out under the mode of constant voltage. During the treatment, titanium samples and stainless steel plate were used as the anode and cathode, respectively. Air pump was opened to agitate the electrolyte and increase the dispersion of SiC particles. The electrolyte temperature were kept below 40 °C by a circulating cooling system. The microstructure, phase composition and tribological properties of MAO TiO₂ coating before and after the incorporation of SiC particles were investigated using SEM, XRD, confocal microscope and ball-on-plate tribometer test.

The TiO₂/SiC composite coating was successfully fabricated by the micro-arc oxidation treatment of titanium in the electrolyte containing SiC submicron particles. Results show that submicron SiC particles dispersed in the MAO electrolyte were incorporated into the TiO₂ coating during the MAO process and the fabricated TiO₂/SiC composite coating mainly consisted of rutile, anatase, and SiC phases. The pore size and surface roughness of TiO₂/SiC composite coating decreased with the increasing addition amount of SiC particles in the electrolyte. Furthermore, the incorporation of SiC particles in the TiO₂ coating suppressed the initiation and propagation of micro-cracks. The dispersed SiC particles in the matrix of composite coating have the function of pinning and strengthening, which improves the mechanical properties of the MAO composite coating. In addition, the incorporation of SiC particles in MAO coating effectively suppressed micro-cracks formation and decreased the coating internal defects. The tribological test of coatings against GCr15 stainless steel balls show that the incorporation of submicron SiC particles in the MAO TiO₂ coating decreased the friction coefficient and wear rate.

Keywords: titanium, micro-arc oxidation, SiC particles, tribological property, composite coating introduction

Erosion test of electroless deposited Ni-Fe-P alloy coatings

Shaofeng Zhu¹, Yixian Li², Chuanqi Chen³

(1. Energy Saving Institute of Anhui Jianzhu University; 2. Anhui Jianzhu University;
3. Anhui Zhongrui Quality Inspection Co., Ltd.)

Abstract: The Ni-Fe-P alloy coatings were prepared by electroless plating on pure copper, and erosion test of the coatings in liquid-solid two-phase flow was investigated by self-design experimental facility. The microscopic morphology of the samples under different conditions was analyzed by scanning electron microscope. The results are drawn as follows. In the 3.5wt% NaCl suspension system, when the flow rate is constant, as the particle size increases, the mass loss of coatings increase at first and then decrease in the test range of impact angles. The mass loss of the coating reaches the maximum near the particle size of 120 meshes. Under the joint action of shear and shock, the small holes in the sample surface increase gradually with the impact angle increasing. When the particle size is 60 meshes or 120 meshes, the mass loss of the sample increases with the impact angle increasing. Analysis by scanning electron microscopy shows that when the impact angle is 45 degrees, the surface of the sample has a marked scratch, and the damnification is more serious; the small holes are found on the surface of the sample, when the impact angle increases to 90 degrees. Keeping the impact angle at 45 degrees, when the particle size is 60 meshes or 240 meshes, the mass loss of the coatings increasing slowly with the flow rate increasing. When the particle size is 120 meshes, the mass loss of the coating increases significantly with the flow rate increasing. By scanning electron microscope analysis, it can be found that when the flow rate is 50 mL/s, the severity of the surface morphology of the coatings increase and then decrease with the particle size increasing of the samples; the cutting marks on the surface of the coating are obvious, when the particle size is 60 meshes or 120 meshes; the small pores on the surface of the coating are found, when the size of the particles reaches 180 meshes.

In the 5wt% NaOH suspension system, when the flow rate is constant, the mass loss of the coating is almost the same as that in the 3.5wt% NaCl suspension system in the test range of impact angles, as the particle size increases, the mass loss of coatings increase at first and then decrease in the test range of impact angles. The mass loss of the coating reaches the maximum near the particle size of 120 meshes. However, when the particle size is 60 meshes, the mass loss of the sample decreases with the impact angle increasing. Keeping the impact angle at 45 degrees, when the particle size is 60 meshes, 120 meshes or 240 meshes, the mass loss of the coatings increases significantly with the increase of flow rate. In the 5vol% HCl suspension system, the erosion rules become more complex. Keeping the flow rate constant, when the impact angle is 45 degrees, 60 degrees or 75 degrees, the mass loss of coatings increase with the particle size increasing and then decrease. The mass loss of the coating reaches the maximum near the particle size of 180 meshes. Through the scanning electron microscope analysis, it can be seen that the damage of the coating is obviously aggravated with the decrease of particle size.

In conclusion, the corrosion resistance of electroless Ni-Fe-P coating in 5wt% NaOH suspension system is best than that in others, while the corrosion resistance in 5vol% HCl suspension system is significantly worse than that in others.

Keywords: electroless plating, Ni-Fe-P alloy, erosion, coating

Effect of different heat treatment time on wear performance of

Al₂O₃-13wt%TiO₂ coating

Chao Liu, Sanming Du
(Henan University of Science and Technology)
dsming@haust.edu.cn

Abstract: The work aims to explore the effect of different heat treatment time on wear performance of Al₂O₃-13wt%TiO₂ coating. Air plasma spraying system was utilized to deposit Al₂O₃-13wt%TiO₂ (AT13) coatings on 20 steel samples. Commercial micron AT13 powder was used with a particle size of 40-60 μm. 20 steel plate with the dimensions of φ75 mm×8 mm was selected as the substrate. Plasma spray process was carried out in air using ZB-80 plasma spraying equipment. Before process the samples were sand-blast in accordance with conventional method. The thicknesses of the ceramic coating were approximately 0.4 mm. After plasma spraying the coatings were heat treated at 500 °C different times i.e. 1, 3, 5 h. The microstructures, microhardness and phase compositions of the coatings were investigated by scanning electron microscopy, microhardness tester and X-ray diffraction, respectively. Test the friction and wear performance of coatings with QG-700 friction and wear tester. The results indicate that coating is mainly composed of Al₂O₃, TiO, Al₂TiO₅ and AlN phases. The heat treatment does not change the phase composition of the coating. The reason is that the heat treatment temperature does not reach the critical phase transition temperature and the holding time is insufficient. The bonding method between the substrate and the coating is mainly mechanical bonding. The interior of the coating is a lamellar structure. No significant change in the microstructure of the coating before and after heat treatment. The coating consists of completely melted melt structure, unmelted particles and pores. The reasons causing this complex structure can be explained as follows: as the powders are sent to the surface in the plasma flow after exposed to heat for a very short period of time some of the particles completely melt and deposit onto the surface, some particles remain on the surface as unmelted particles. Another reason is that there may be stresses on the microstructure due to the shrinkage of the splats sprayed individually throughout the fast cooling. The heat treatment reduces the microhardness of the coating and the microhardness was the lowest at 500 °C-3 h. The reason is that the heat treatment reduces the residual stress of the coating and therefore the microhardness decreases. The friction coefficient of the coating after heat treatment has been improved, the friction coefficient increases least after heat treatment for 3 hours and the friction process is divided into two stages: the initial stage of friction and the friction stabilization stage. After the friction and wear test, the untreated and heat-treated coatings had wear debris, micro-cracks and exfoliation pits. The wear mechanisms of the four coatings are the same but the degree of wear decreases with the increase of the holding time and the width of wear marks decreases as the heat treatment time increases. With the increase of holding time, the wear rate showed a decreasing trend. After a long time of and heat treatment the coating releases some residual stress. The element diffusion and grain growth fill some of the pores, which increases the density of the coating, reduces the probability of cracks and reduces the wear rate of the coating. The wear rate was the lowest at 500 °C-5 h.

Keywords: plasma spraying, heat treatment

A highly porous thermal barrier coating based on

Gd₂O₃-Yb₂O₃ Co-doped YSZ

Kirsten Bobzin, Lidong Zhao, Mehmet Öte, Tim Königstein

(Surface Engineering Institute, RWTH Aachen University Kackertstr. 15, 52072 Aachen, Germany)

zhao@iot.rwth-aachen.de

Abstract: Co-doped zirconia based thermal barrier coatings (TBCs) have been found to possess lower thermal conductivity and higher sintering resistance at high temperatures than current state of the art ZrO₂-(7-8)wt%Y₂O₃. In this study, a highly porous TBC based on Gd₂O₃-Yb₂O₃ co-doped YSZ was produced using a special spray powder prepared by high energy ball milling with a three-cathode plasma generator TriplexProTM-210. The coating was characterized in terms of the microstructure, phase composition, hardness and thermal conductivity. The thermal shock behavior was evaluated using thermal cyclic test at $T=1,150$ °C. A free-standing coating was heat-treated in a furnace at $T=1,150$ °C for $t=500$ h to investigate the effect of sintering on the microstructure and properties of the coating. Results revealed that the coating in as-sprayed condition exhibited a highly porous microstructure with a porosity of $p=39\%$. The highly porous TBC presented a better thermal shock behaviour compared to a conventional TBC. After heat-treatment, the value of porosity amounted to $p=26\%$, representing a highly porous microstructure. Both the thermal conductivity and hardness of the coating significantly increased due to sintering. However, the coating exhibited low thermal conductivity values of $\kappa < 1.1$ W/m K at high temperatures.

Keywords: thermal barrier coating, high energy ball milling, thermal shock behaviour, microstructure, thermal conductivity

Development of a FeCrMnBC-based economical wear and

corrosion resistant coating

Kirsten Bobzin, Lidong Zhao, Mehmet Öte, Tim Königstein

(Surface Engineering Institute, RWTH Aachen University, Kackertstr. 15, 52072 Aachen, Germany)

zhao@iot.rwth-aachen.de

Abstract: Main advantages of Fe-based coatings are their favourable lower costs as well as their good environmental behaviour compared to other established protective coatings. In this study, a highly economical coating system based on a FeCrMnBC alloy was developed, consisting only of economically favourable elements. The coating was produced using a spray powder with a size distribution of $-90+45$ µm by a three-cathode plasma generator TriplexProTM-210 and evaluated in terms of the microstructure, hardness, wear and corrosion resistance. It was found that the coating exhibited a dense lamellar microstructure and a microhardness value of more than 600 HV0.1. The coating was significantly more wear resistant compared with a plasma sprayed stainless steel coating of 316 L. Salt spray test confirmed that the corrosion behavior of the FeCrMnBC coating was comparable to that of a plasma sprayed 316 L coating. Due to the higher wear resistance, comparable corrosion behavior and lower material costs this new coating system can be used as more economical alternative or replacement to conventional stainless steel coatings to protect carbon steel as well as cast iron parts against wear and corrosion.

Keywords: Fe-based coating, plasma spraying, microstructure, wear, corrosion

Study on the transfer behavior of polyimides adding aluminum rubbing with Ti-6Al-4V alloy at different temperatures

Ruoyu Liu, Zhiguang Wang, Chuanbing Huang, Hao Lan, Weigang Zhang
(Institute of Process Engineering, Chinese of Academy)
wgzhang@home.ipe.ac.cn

Abstract: The friction transfer behavior between the Ti-6Al-4V alloy and polyimide-Al composite coating was studied from 373 K to 773 K with a high temperature tribometer equipment. Through the vacuum hot pressing, the polyimide and the aluminum were pressed into the coating. The friction coefficient of the process was about 0.3 at the different temperature. The wear mechanism of the Ti-6Al-4V alloy and polyimide-Al was abrasive wear below 573 K. Above 573 K, the transfer layer would formation on the surface of the Ti-6Al-4V alloy. The addition of the aluminum materials strengthened the binding between the transfer layer and the Ti-6Al-4V alloy above 573 K. Remarkably, the wear mechanism was transfer to the adhesive wear. The addition of the aluminum would also increase the amount of the transfer layer.

Keywords: Ti-6Al-4V, polyimide, aluminum, friction, transfer behavior

Effect of nano-additives containing rare earth oxides on impact abrasive wear behavior of high chromium cast irons

Xiaochun He¹, Ruiqing Chu¹, You Wang², Xiaohong Xing²
(1. School of Environmental and Material Engineering, Yantai University;
2. Department of Materials Science, Harbin Institute of Technology)
hexiaochun76@126.com

Abstract: High chromium cast irons (HCCIs) with nano-additives were prepared. The X-ray diffractometer (XRD) was employed to analyze the phase compositions. The hardness and impact toughness were measured by a Rockwell hardnessmeter and an impacting test enginey. The friction and wear behavior of HCCIs in different conditions were investigated using an abrasive wear tester. And then, the morphology of the wore specimen was studied by a scanning electronic microscope (SEM). The experimental results showed that nano-additives increased the hardness and the impact toughness. The hardness of HCCIs with nanoadditives is 58.3 HRC, which increased by 5.0% than that of HCCIs without nano-additives. The toughness of HCCIs with nano-additives is 7.83 J/cm², which increased by 23.9% than that of HCCIs without nano-additives. At the low impact energy (2 J), nano-additives deteriorated the resistance of the impact abrasive wear. The wear mechanism was the gouging abrasion and cutting wear. At the high impact energy (5 J), nano-additives improved the resistance of the impact abrasive wear. The wear mechanism was fatigue wear and plastic deformation wear, supplemented by crack propagation and gouging abrasion.

Keywords: high chromium cast irons, nano-additives, impact abrasive wear, wear mechanism

Effect of flow velocity on erosion-corrosion rate of mild steel in solid-liquid two phase fluids comprising CO₂ and Cl⁻ environments

Lu Cui, Yihua Dou, Zhen Li
(School of Mechanical Engineering, Xi'an Shiyou University)
lizhenxysu@sina.com.cn

Abstract: Effect of flow velocity and mean impact angle on the erosion-corrosion(E-C) rate of 13Cr steel for oilfield ground gathering transferring system was studied through experiments. The tests were performed using three kinds of solid-liquid two-phase flow (3.5% NaCl aqueous solution, saturated CO₂ aqueous solution and CO₂+3.5% NaCl aqueous solution respectively mixed with quartz grain with 210 μm to 420 μm in diameter). The surface morphology of specimen suffer from E-C is analyzed by scanning electron microscopy (SEM). The research confirm that the E-C rate increased exponentially with the increase of flow velocity. The equation $V_e=KV_n$ can be used to express the relationship between E-C rate and flow velocity. Furthermore, it is suggested that the experimental results can be divided into two parts, lower velocity and higher velocity section. Using equation $V_e=KV_n$ 'segment fitting' method has higher fitting precision. The analysis of experimental results and SEM surface topography show that the material removal rate is controlled by electro-chemical corrosion at lower flow velocity and may suffer from mechanically induced deterioration at higher flow velocity. The impact angle has complex effects on E-C rate. In the experiment situation, the E-C rate at lower impact angle is larger than which at higher impact angle and will reach highest at 45 °impact angle.

Keywords: erosion-corrosion, solid-liquid two-phase, mild steel

Research on laser surface strengthening of U71Mn steel based on resistance of the sand erosion

Jingfeng Lei, Wenjun Qi, Yadong Xie, Yanhua Huang
(Xinjiang University)
wenjuntsi@163.com

Abstract: Aiming at the wind erosion situation of the LanXin high-railway in gale areas, research on laser melting and laser cladding U71Mn steel specimens, obtain the functional layers and analyze the microstructure, hardness and so on. Research the surface friction wear and erosion after laser cladding. The results indicate that the laser power of 1300 W, scanning speed of 4 mm/s, off-focus length 8 mm, phase transformation zone has the maximum hardness of 1079 HV, which is 3.6 times of the matrix. The microstructure of fused zone and phase transformation zone consists of martensite columnar, and the microstructure of heat affected zone consists of mixing the martensite, troostite and residual austenite. MnSFeO low-melting-point eutectic appears at the junction of the fused zone and phase transition zone and results in hot crack. The optimum parameters of laser cladding with 25% WC/Ni powder and 50% overlapping rate are: laser power is 1500 W, scanning speed is 6mm/s, powder feed rate is 1 r/min, off-focus length is 0 mm, cladding layer is smooth without cracks, impurities and air bubbles, and the highest hardness is 1170 HV, which is 3.7 times of the matrix. The wear quantity of the matrix is 5 to 10 times of cladding layer's. The pit of cladding layer is obviously smaller than that of the matrix. The surface friction and erosion wear resistance is effectively improved as U71Mn steel specimens treated with laser cladding.

Keywords: the high-speed rail, sand erosion, laser melting, laser cladding

Elevated temperature wear behaviour of rare earth modified WC12Co coating

Yan Liu, Guiying Yang, Zongqiu Hang, Hao Fu, Naiyuan Xi, Hui Chen
(Southwest Jiaotong University)
liuyanzt@163.com

Abstract: WC-Co coating prepared by HVOF technology has been widely applied in many fields for its high hardness and excellent friction wear properties. However, with the increasing requirement of high temperature wear resistance for the components, conventional WC-Co coating cannot satisfy the application. Additives of rare earth is supposed to be an effective method to improve high temperature properties for its grain boundaries strengthening effect on the coatings and contribution to change the mechanism of oxide film growth, which can effectively improve mechanical properties of the coatings. The high temperature wear tests of conventional, nano and bi-modal WC-12Co coatings were conducted by many researchers. Relationships between microstructure and wear properties and wear mechanisms were discussed. However, high temperature sliding behavior and the related mechanism of WC-Co coatings with rare-earth addition were seldom investigated. In the present study, CeO₂ modified WC-12Co coatings were prepared by high velocity oxygen flame spraying (HVOF) technology. The dry sliding wear tests were conducted on a pin-on-disk tribometer (MMU-5G), and the KmTBCr26 pin with diameter of 4 mm was adopted as counterpart. The sliding wear tests were conducted at an invariable load of 100 N, sliding velocity of 300 r/min, and an high temperature setting at 450, 550 and 650 °C. Weight loss of the coatings was measured, and friction coefficient was recorded by the computer. The morphologies of worn tracks were observed by scanning electron microscope (SEM) every 1 h to investigate the wear mechanisms. The results show that the mass loss rate of the coating worn at 450 °C increases first and then decreases. When at 550 °C, it displays the tendency of decreasing to increasing and finally to decreasing. The wear loss rate demonstrates decline tendency with wearing time from 1h to 4h when wearing at 650 °C. The lowest wear loss rate of the coatings at different sliding wear temperature are all obtained after 4h wearing. The wear mechanism is different at the temperature of 450, 550 and 650 °C. Slight abrasive wear dominates the wear mechanism at 450 °C and 550 °C. Abrasive wear dominates the wear mechanism supplemented by oxidation wear at 650 °C.

Keywords: CeO₂ modified WC-12Co coating, dynamic process, elevated temperature wear mechanism

Effect of mechanical alloying speed on properties of CNTs-SiC/Ni laser cladding coating

Longzhi Zhao
(School of Materials Science and Engineering)
245145007@qq.com

Abstract: CNTs-SiC/Ni surface reinforced coatings were prepared by laser cladding with composite powders mixed by high-energy planetary ball mill. The effects of mechanical alloying speed on the microhardness and wear resistance of CNTs-SiC/Ni were studied. The results show that with the mechanical alloying speed increases, the hardness of the coating increases first and then decreases, the wear volume presents the first decrease, the friction coefficient of the coating before finally tends to be stable, and finally the fluctuation increases. And the hardness is the highest when the mechanical alloying speed reaches 300 r/min, the friction coefficient and the wear ratio of the ratio of λ value reaches the maximum, and the friction performance is the best.

Keywords: laser cladding, friction performance, mechanical alloying, carbon nanotubes, agglomeration